Direct Cavity Detection of Majorana Pairs

Matthieu C. Dartiailh,[1] Takis Kontos,[1] Benoit Douçot,[2] and Audrey Cottet[1]
[1]*Laboratoire Pierre Aigrain, Ecole Normale Supérieure-PSL Research University, CNRS, Université Pierre et Marie Curie-Sorbonne Universités, Université Paris Diderot-Sorbonne Paris Cité, 24 rue Lhomond, 75231 Paris Cedex 05, France*
[2]*Sorbonne Universités, Université Pierre et Marie Curie, CNRS, LPTHE, UMR 7589, 4 place Jussieu, 75252 Paris Cedex 05, France*
(Received 11 July 2016; published 23 March 2017)

No experiment could directly test the particle-antiparticle duality of Majorana fermions, so far. However, this property represents a necessary ingredient towards the realization of topological quantum computing schemes. Here, we show how to complete this task by using microwave techniques. The direct coupling between a pair of overlapping Majorana bound states and the electric field from a microwave cavity is extremely difficult to detect due to the self-adjoint character of Majorana fermions which forbids direct energy exchanges with the cavity. We show theoretically how this problem can be circumvented by using photoassisted tunneling to fermionic reservoirs. The absence of a direct microwave transition inside the Majorana pair in spite of the light-Majorana coupling would represent a smoking gun for the Majorana self-adjoint character.

DOI: 10.1103/PhysRevLett.118.126803

Majorana quasiparticles are among the most intriguing excitations predicted in condensed matter physics [1]. The Majorana particle is equal to its own antiparticle, a property which opens up possibilities of non-Abelian statistics [2] and topologically protected quantum computation [3] in condensed matter systems. Low-frequency conductance measurements have prevailed so far in the experimental search for these exotic quasiparticles. In particular, hybrid structures combining semiconducting nanowires and superconductors have been intensively investigated [4,5]. The recent observation of zero-energy conductance peaks and pairs of peaks with an oscillatory splitting is consistent with the existence of Majorana bound states (MBSs) [6–11]. However, it is essential to find new tools to test more specifically the nature of these peaks [12–17].

Paradoxically, the self-adjoint character of MBSs, which draws so much interest, also makes them very difficult to detect. Photons trapped in a high-finesse cavity are *a priori* very appealing for probing these elusive excitations [18]. Indeed, light, contrarily to conductance measurements, preserves the occupation number encoded into a pair of MBSs. Unfortunately, for the same reason, a pair of MBSs cannot exchange energy with an electromagnetic field, which forbids any direct spectroscopy. This seems to limit the use of light [19–24]. Recently proposed quantum computing architectures rely on an indirect MBS-photon coupling through a metallic Josephson circuit [25–32].

In this theoretical work, we show that the imperfections of a realistic Majorana nanocircuit, although undesirable for quantum information applications, can be exploited at present to characterize MBSs with microwave techniques. First, a realistic Majorana nanocircuit must have a finite size to remain in the coherent regime. Therefore, MBSs can have a spatial overlap. This naturally generates, for a pair of MBSs, an energy splitting 2ε and a *direct* coupling β to the cavity electric field [20,33]. Second, the presence of even a tiny amount of zero-energy quasiparticles in superconducting or normal metal contacts, which is inherent to experimental setups demonstrated so far, switches on photoassisted tunnel processes which involve only one partner of a Majorana doublet. During these transitions, photons with frequency ε are exchanged between the cavity and the Majorana pair, with a rate set by β. However, transitions at frequency 2ε remain forbidden regardless of the circuit parameters. The purely longitudinal nature of β, thereby revealed, would represent a direct signature, in the simplest setup, of the self-adjoint character of MBSs.

Hybrid nanocircuits with superconducting parts have been coupled very recently to microwave cavities [34–37]. The light-matter coupling in such devices can be described generically with the Hamiltonian

$$\hat{h}_{\rm tot} = \hat{h}_{\mathcal{N}} + \omega_0 \hat{a}^\dagger \hat{a} + \hat{h}_{\mathcal{C}}(\hat{a} + \hat{a}^\dagger) \tag{1}$$

with ω_0 the cavity frequency. In a typical experiment, one determines the cavity frequency pull $\Delta\omega_0$ and damping pull $\Delta\Lambda_0$ from the cavity microwave response measured at frequency $\omega_{\rm rf} = \omega_0$. In the case of an electric coupling scheme, from a semiclassical linear response description, these signals correspond to $\Delta\omega_0 + i\Delta\Lambda_0 = \chi(\omega_0)$, with χ^* the nanocircuit charge susceptibility [35]. In a first approach, one can assume that the nanocircuit spectrum is discrete. Since $\hat{h}_{\mathcal{N}(\mathcal{C})}$ are quadratic, one can use $\hat{h}_{\mathcal{N}} = \sum_\alpha E_\alpha \gamma_\alpha^\dagger \gamma_\alpha$ and $\hat{h}_{\mathcal{C}} = \sum_\alpha M_{\alpha\beta}\hat{\gamma}_\alpha^\dagger\hat{\gamma}_\beta + N_{\alpha\beta}\hat{\gamma}_\alpha^\dagger\hat{\gamma}_\beta^\dagger + N_{\alpha\beta}^\dagger\hat{\gamma}_\alpha\hat{\gamma}_\beta$, with $E_\alpha > 0$, $\hat{\gamma}_\alpha^\dagger$ Bogoliubov operators which combine

electron and hole excitations, and $\{M_{\alpha\beta}, N_{\alpha\beta}\}$ matrix elements which depend on the overlap of the cavity photonic pseudopotential with the wave functions associated with $\hat{\gamma}^\dagger_{\alpha(\beta)}$ [33]. At zero temperature ($T = 0$), this gives $\chi^*(\omega_0) \simeq \sum_{\alpha\beta} |N_{\alpha\beta}|^2 (\omega_0 - E_\alpha - E_\beta + i0^+)^{-1}/2$. Importantly, due to the Pauli exclusion principle, one has $N_{\alpha\alpha} = 0$. Hence, $\chi(\omega_0)$ does not involve transitions between electron and holes associated with conjugated operators $\hat{\gamma}^\dagger_\alpha$ and $\hat{\gamma}_\alpha$. This selection rule can be extended to $T \neq 0$ or a level broadening smaller than the interlevel separation [38]. However, having a nanocircuit response at $\omega_0 = 2E_\alpha$ is possible provided there exists a state degeneracy $E_\alpha = E_{\alpha'}$ in the nanocircuit [38], as observed in spin-degenerate superconducting atomic contacts [34,44]. In contrast, lifting degeneracies is crucial to obtain MBSs. In elementary models [4,5], when a finite portion of a nanoconductor is driven to its topological phase, one nondegenerate Bogoliubov doublet $(\hat{\gamma}^\dagger_1, \hat{\gamma}_1)$ approaches alone the zero-energy area to form a pair of MBSs described by self-adjoint creation operators $\hat{m}_L = (\hat{\gamma}^\dagger_1 + \hat{\gamma}_1)/\sqrt{2}$ and $\hat{m}_R = i(\hat{\gamma}^\dagger_1 - \hat{\gamma}_1)/\sqrt{2}$ such that one has, at low energies, $\hat{h}_{\mathcal{N}} = \varepsilon \hat{\gamma}^\dagger_1 \hat{\gamma}_1 = i\varepsilon \hat{m}_L \hat{m}_R + (\varepsilon/2)$ with $\varepsilon = E_{11}$. An important signature of this scenario is the absence of direct microwave transitions in the Majorana subspace, i.e., $\chi(\omega_0 = 2\varepsilon) \simeq 0$ due to $N_{11} = 0$. Remarkably, this occurs even when the Majorana-cavity coupling is finite; i.e., $\hat{h}_C$ contains a term in $i\beta \hat{m}_L \hat{m}_R$ with $\beta = M_{11}$. Using a spin analogy, the cavity and the MBSs can have only a longitudinal coupling, which is not able to change the state of the Majorana pair; i.e., $\hat{h}_C$ and $\hat{h}_{\mathcal{N}}$ are represented by collinear vectors in the Bloch sphere associated with the Majorana subspace. This gives a smoking gun for the nondegenerate $(\hat{\gamma}_1, \hat{\gamma}^\dagger_1)$ electron-hole conjugated pair or, equivalently, the pair of self-adjoint excitations $(\hat{m}_L, \hat{m}_R)$. Importantly, the absence of direct microwave transitions in the Majorana doublet is meaningful only if one can confirm $\beta \neq 0$. Furthermore, the absence of direct transitions should be robust when the control parameters of the nanocircuit are varied, to discard any accidental cancellation of $\chi(\omega_0)$. We use below a specific example to show how these tasks can be achieved.

We now consider a semiconducting nanowire subject to spin-orbit coupling and a Zeeman field. The nanowire is tunnel coupled along its whole length to a superconducting contact S. It is also coupled at both ends to normal metal contacts N_L and N_R, which enable the measurement of the nanowire density of states $\nu(\omega)$. We describe this circuit with a phenomenological one-dimensional tight-binding chain $\hat{h}_{\mathcal{W}} = \sum_n \{\hat{d}^\dagger_n (E_z \hat{\sigma}_z - \mu \hat{\sigma}_0) \hat{d}_n - [\hat{d}^\dagger_n (t\hat{\sigma}_0 + \Lambda \hat{\sigma}_y) \hat{d}_{n+1} + \text{H.c.}]\}$ with $\hat{d}^\dagger_n = \{d^\dagger_{n\uparrow}, d^\dagger_{n\downarrow}\}$ and $d^\dagger_{n\sigma}$ the creation operator for an electron with spin σ in site $n \in [1, N_c]$ of the chain [Fig. 1(a)]. We denote by E_z the Zeeman field on the sites, μ the sites chemical potential, which can be tuned with a gate

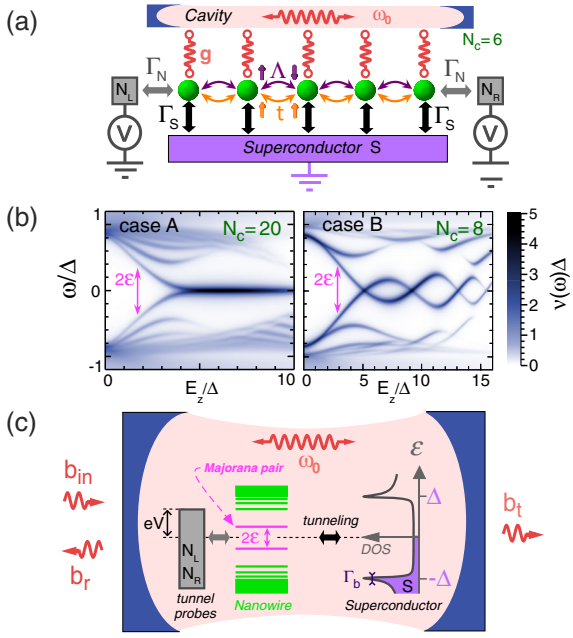

FIG. 1. (a) Tight-binding model of our nanocircuit with $N_c = 6$ sites (green dots). The consecutive sites are coupled by a tunnel-hopping constant t and spin-orbit terms Λ. All sites are tunnel coupled to the superconductor S with a rate Γ_S. The extremal sites are tunnel coupled with a rate Γ_N to normal metal contacts $N_{L(R)}$ with a bias voltage V. All sites are coupled to the microwave cavity with a constant g. (b) DOS $\nu(\varepsilon)$ at the ends of the chain or nanowire, versus ω and E_z, for cases A (long nanowire with negligible coupling to $N_{L(R)}$) and B (short nanowire and coupling to $N_{L(R)}$ and S similar at zero energy). (c) Energetic scheme of the nanocircuit placed in the microwave cavity. The DOS in S depends on the superconducting gap Δ and the broadening parameter Γ_b. The cavity microwave transmission b_t/b_{in} or reflection b_r/b_{in} is measured.

voltage, t the hopping constant between the sites, and Λ the spin-orbit constant. So far, studies on MBSs coupled to cavities have reduced the effect of S to an effective pairing term added to $\hat{h}_{\mathcal{W}}$ [19–22]. However, a realistic model must also take into account level broadening and dissipation. Therefore, we describe explicitly tunneling to S and $N_{L(R)}$ with a Hamiltonian $\hat{h}_{\mathcal{R}}$ (see [38] for details). This leads us to introduce the tunnel rate Γ_N between site $1(N_c)$ and contact $N_{L(R)}$ and the tunnel rate Γ_S between site $n \in [1, N_c]$ and contact S. The DOS of S depends on the superconducting gap Δ but also on a phenomenological parameter Γ_b which accounts for a broadening of the BCS peaks and a finite low-energy DOS [Fig. 1(c)]. Such effects can be caused by a finite magnetic field [45,46]. We consider short chains and choose parameters such that few subgap levels are visible in the DOS of the nanowire, like in recent experiments [10,11]. More precisely, for case A, one has $N_c = 20$, $t = 2.5\Delta$, $\Lambda = 5\Delta$, $\Gamma_b = 0.1\Delta$, $\Gamma_N = 0.001\Delta$, and $\mu = 6\Delta$, and, for case B, one has $N_c = 8$, $t = 5\Delta$, $\Lambda = 4\Delta$, $\Gamma_b = 0.05\Delta$, $\Gamma_N = 0.2\Delta$, and $\mu = 5.5\Delta$. We use $E_z = \Delta$, $\Gamma_S = 5.5\Delta$, and $k_B T = 0.01\Delta$

for both cases. The density of states $\nu(\omega)$ at the ends of the nanowire reveals the occurrence of a pair of MBSs above a critical Zeeman field [Fig. 1(b)]. These MBSs show an oscillatory energy splitting with E_z and μ for a very short chain (case B) or stick to zero energy for a longer chain (case A) [47].

We assume that the above nanocircuit is embedded in a microwave cavity. Hence, we use Hamiltonian $\hat{h}_{\rm tot}$ of Eq. (1) with $\hat{h}_{\mathcal{N}} = \hat{h}_{\mathcal{W}} + \hat{h}_{\mathcal{R}}$ and $\hat{h}_{\mathcal{C}} = g\sum_n \hat{d}_n^\dagger \hat{d}_n$. This last term means that cavity photons modulate the chemical potential of site n with a coupling constant g [33]. To treat on the same footing internal nanowire transitions and tunneling to the reservoirs, we use a Keldysh approach [35,44,48–50]. We use Python and Numba, a Python compiler based on the LLVM compiler infrastructure project [51], to calculate numerically $\Delta\omega_0 + i\Delta\Lambda_0 = \chi(\omega_0)$ with [35]

$$\chi^*(\omega_0) = -ig^2 \int \frac{d\omega}{4\pi} \mathrm{Tr}[\check{\mathcal{S}}(\omega)\check{\mathcal{G}}^r(\omega)\check{\Sigma}^<(\omega)\check{\mathcal{G}}^a(\omega)] \quad (2)$$

and $\check{\mathcal{S}}(\omega) = \check{\tau}[\check{\mathcal{G}}^r(\omega+\omega_0) + \check{\mathcal{G}}^a(\omega-\omega_0)]\check{\tau}$. Above, the retarded and advanced multisite Green's functions $\check{\mathcal{G}}^{r/a}$ and the lesser self-energy $\check{\Sigma}^<(\omega)$ can be calculated from $\hat{h}_{\mathcal{N}}$, while $\check{\tau}$ takes into account the structure of the photon-particle coupling in the Nambu⊗spin space [38].

We focus on the dissipative response $\Delta\Lambda_0 = \mathrm{Im}[\chi(\omega_0)]$ of the cavity, which should naturally reveal the effects of dissipative reservoirs. We first consider case A, where $\varepsilon \to 0$ in the topological phase of the nanowire. The $\omega_0 - E_z$ map of $\mathrm{Im}[\chi(\omega_0)]$, shown in Fig. 2(a) with $\omega_g = g^2/\Delta$, reveals a wealth of features, sketched in Fig. 2(b). Feature ① is shown in more detail in Fig. 2(c) for constant values of ω_0. It consists of a step at $\omega_0 = \varepsilon$, which is the energy distance between one MBS and the Fermi level of the reservoirs. For case A, the effects of the $N_{L(R)}$ reservoirs on χ can be disregarded due to the vanishing Γ_N. Therefore, feature ① can be attributed to photoinduced tunneling between the MBSs and the residual subgap DOS of S, as represented in Fig. 2(d) ①. In practice, it is possible to have a well-grounded S contact by realizing a direct connection between S and the cavity ground plane [35,52]. In this case, feature ① can exist only if the MBSs are directly coupled to cavity photons, i.e., $\beta \neq 0$. In spite of this coupling, no transition occurs at $\omega_0 = 2\varepsilon$ [red dotted line in Fig. 2(b)]. The simultaneous presence or absence of a step or resonance at $\varepsilon(2\varepsilon)$ occurs on a wide range of E_z. We have therefore obtained a signature of the Majorana self-adjoint character [54]. More precisely, these features indicate that we are in presence of a nondegenerate electron-hole conjugated pair, which is the natural precursor of a Majorana pair. It is then important to check from $\nu(\omega)$ that ε vanishes with E_z (or shows several zero-energy crossings), as a signature of the spatial isolation of the two MBSs formed out of the nondegenerate electron-hole pair.

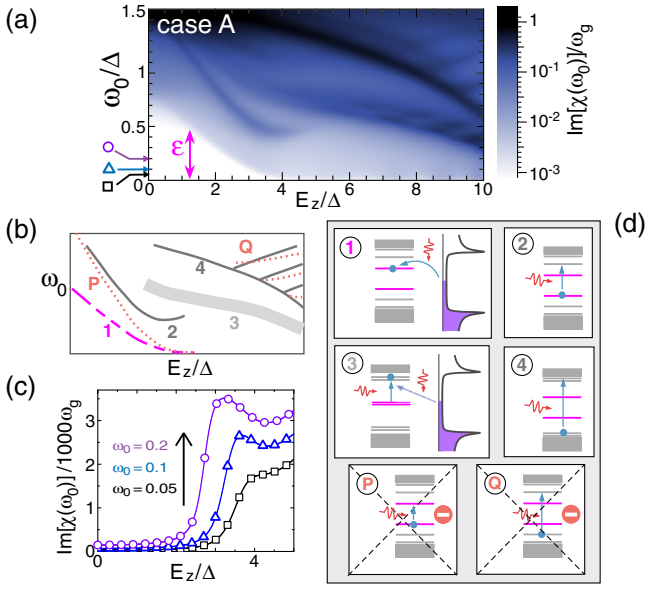

FIG. 2. (a) $\mathrm{Im}[\chi(\omega_0)]$ versus ω_0 and E_z for case A with $V = 0$. (b) Scheme of the main features appearing in panel (a). (c) $\mathrm{Im}[\chi(\omega_0)]$ versus E_z for constant values of ω_0 corresponding to the symbols in panel (a). (d) Processes contributing to the features of panel (b) and forbidden processes P and Q.

We now demonstrate the robustness of our main results to variations of the nanowire spectrum. Figure 3(a) shows the $\omega_0 - E_z$ map of $\mathrm{Im}[\chi(\omega_0)]$ in the case of a shorter nanowire (case B). Feature ① persists in this limit, as indicated by the pink circle. Besides, the yellow circles indicate new steps caused again by photoassisted tunneling from or to the MBSs at $\omega_0 = \varepsilon$. These steps can have a contrast significantly stronger than feature 1. Meanwhile, no resonant feature is visible along the $\omega_0 = 2\varepsilon$ contour indicated by the red dotted line. This extends the possibilities for testing the longitudinal character of the coupling between the Majorana doublet and the cavity. Importantly, feature 1 of case A has an amplitude of $3 \times 10^{-3} g^2/\Delta$. With $\Delta = 180$ μeV and a site-cavity coupling $g = 2$ μeV, this corresponds to 15 kHz. The pink circle features of case B have an amplitude of $6.3 \times 10^{-2} g^2/\Delta$, which corresponds to 340 kHz. These signals are small but within experimental reach [55,56], although the residual zero-energy DOS in S is small, i.e., $r \sim 5\%$ (2.5%) in case A (B), which leads to the "hard gap" situation similar to Ref. [57]. Note that, in case B, tunneling quasiparticles can be provided by both the S and $N_{L(R)}$ reservoirs, which contribute similarly to the broadening of the low-energy MBSs due to our choice of parameters. We will see later how to distinguish these contributions thanks to a finite bias voltage. Noticeably, an isolated zero-energy crossing of two ordinary Andreev bound states could be caused by a trivial spin-degeneracy lifting. However, in this case, the frequency of feature ②, which corresponds to an internal nanowire transition inwards or outwards the pair, will not depend on E_z,

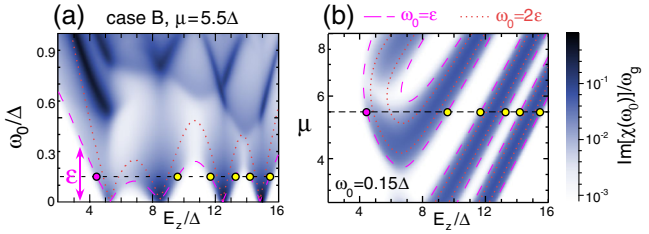

FIG. 3. (a) $\mathrm{Im}[\chi(\omega_0)]$ versus ω_0 and E_z for case B and $V = 0$. (b) Corresponding $E_z - \mu$ map for $\omega_0 = 0.15\Delta$. The pink circle corresponds to feature ① of Fig. 2, while the features with the yellow circles are specific to the short nanowire case.

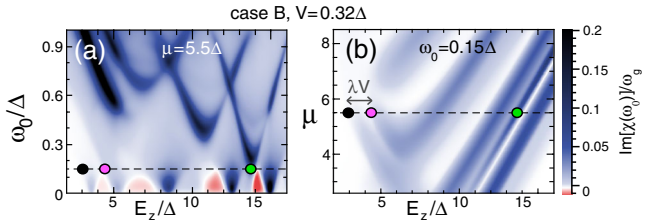

FIG. 4. (a) $\mathrm{Im}[\chi(\omega_0)]$ versus ω_0 and E_z for case B and $eV = 0.32\Delta$. (b) Corresponding $\mu - E_z$ map of $\mathrm{Im}[\chi(\omega_0)]$ for $\omega_0 = 0.15\Delta$.

in contrast to the Majorana case, where it strongly depends on E_z due to the topological phase transition [38]. Therefore, our setup is also able to rule out the case of a trivial superconducting wire with time-reversal symmetry-breaking impurities.

In practice, to measure experimentally signals similar to Figs. 2(a) and 3(a), one must vary ω_0. In principle, this is technically possible [58,59]. However, it is useful to adapt our predictions for standard setups with a fixed ω_0. In this case, other parameters must be changed to characterize the nanocircuit [60]. In Fig. 3(b), we show $\Delta\Lambda_0$ versus E_z and μ, for case A. We use $\omega_0 = 0.15\Delta$, which corresponds, with the gap $\Delta = 180$ μeV of Al, to the value $\omega_0 = 6.6$ GHz compatible with present microwave techniques. In these conditions, $\Delta\Lambda_0$ shows an ensemble of photoassisted tunneling stripes which reveal the well-known oscillations of ε with E_z and μ. The correspondence between Figs. 3(a) and 3(b) is given by the pink and yellow circles. The stripes are absent for low values of E_z, where the nanowire makes the transition to its nontopological phase and the MBSs thus disappear. The $\omega_0 = 2\varepsilon$ contours are shown with red dotted lines in Fig. 3(b). They do not correspond to any remarkable feature in the $\mu - E_z$ map of $\mathrm{Im}[\chi(\omega_0)]$, contrarily to the $\omega_0 = \varepsilon$ contours (pink dashed lines). Importantly, in an experiment, the red and pink contours can be determined independently from any theory, by performing a conductance measurement on $N_{L(R)}$ to get $\nu(\omega)$. We conclude that, in the case where ω_0 cannot be varied, a $\mu - E_z$ map of $\Delta\Lambda_0$ and $\nu(\omega)$ gives an efficient way to characterize the light-matter coupling in our circuit.

We show below that applying a bias voltage to the hybrid nanocircuit-cavity system [61–63] enables one to discriminate processes involving the different fermionic reservoirs and to further check that the MBSs are well coupled to cavity photons. Figure 4(a) shows the $\omega_0 - E_z$ map of $\mathrm{Im}[\chi(\omega_0)]$ for case B, with a finite bias voltage V applied simultaneously to N_L and N_R. We observe clear differences with the case $V = 0$ of Fig. 3(a). First, a new step marked by the black circle appears, due to tunneling between the MBSs and the $N_{L(R)}$ reservoirs, at $\omega_0 = \varepsilon - eV$. Meanwhile, the step marked with the pink circle at $\omega_0 = \varepsilon$ persists and is now due only to tunneling to S. The separation λV between the black and pink circles, which appears for a finite V, is also well visible in the $\mu - E_z$ map of $\mathrm{Im}[\chi(\omega_0)]$ [see Fig. 4(b), where $\lambda \simeq e/\Delta(\partial\varepsilon/\partial E_z)$]. Second, photon emission revealed by $\mathrm{Im}[\chi(\omega_0)] > 0$ appears for $V > \varepsilon + \omega_0$, due to inelastic tunneling between $N_{L(R)}$ and the upper MBS [red areas in Fig. 3(a)]. We conclude that the use of a bias voltage enables a differentiation of the processes involving the $N_{L(R)}$ and S contacts. The persistence of the pink circle feature ensures that cavity photons modulate the potential difference between the MBSs and S. Interestingly, for $V > \varepsilon$, the upper MBS becomes populated, so that internal transitions to upper Andreev levels appear at remarkably low frequencies [see, e.g., green circle in Figs. 4(c) and 4(d)]. This represents another signature of the photon-MBS coupling, although it is not the coupling constant $\beta = M_{11}$ which is involved in this case but rather $N_{1\alpha}$ with $\alpha \neq 1$ and $E_\alpha > \varepsilon$.

In any detection setup, false positive detection events can occur. In our case, a false positive detection of MBSs could happen in the (unlikely) case of a pair of extended nondegenerate Andreev bound states which would have accidentally an energy splitting with the same magnetic field dependence as the nonlocal pair of localized Majorana modes of Fig. 1(b) and a nonconclusive feature 2. To rule out such a situation, one could perform supplementary tests readily accessible in our setup, such as nonlocal transport measurements using the S, N_L, and N_R contacts, with, for instance, a varying pair splitting 2ε (see, for instance, Refs. [69–71]).

In conclusion, we have shown how to exploit photo-induced tunneling to check that a pair of MBSs is directly coupled to cavity photons. However, the direct microwave transitions inside the Majorana subspace remain forbidden in a wide range of parameters. This provides a means to check the self-adjoint character of MBSs. Importantly, this protocol is independent from any theory if the conductance of the nanowire is measured simultaneously with the cavity response to determine $\nu(\omega)$. Such crossed measurements are routinely achieved with mesoscopic QED devices [35,53,62–68]. Our proposal relies on a nanocircuit geometry widely realized experimentally and which has reproducibly revealed low-energy conductance peaks. Furthermore, nanoconductors with superconducting contacts have been coupled to microwave cavities recently [35–37]. Therefore,

our proposal can be straightforwardly implemented with present experimental means.

We thank M. M. Desjardins and L. C. Contamin for useful discussions. This work was financed by the European Research Council Starting grant CirQys.

[1] A. Y. Kitaev, Unpaired Majorana fermions in quantum wires, Phys. Usp. **44**, 131 (2001).
[2] D. A. Ivanov, Non-Abelian Statistics of Half-Quantum Vortices in p-Wave Superconductors, Phys. Rev. Lett. **86**, 268 (2001).
[3] C. Nayak, S. H. Simon, A. Stern, M. Freedman, and S. D. Sarma, Non-Abelian anyons and topological quantum computation, Rev. Mod. Phys. **80**, 1083 (2008).
[4] R. M. Lutchyn, J. D. Sau, and S. D. Sarma, Majorana Fermions and a Topological Phase Transition in Semiconductor-Superconductor Heterostructures, Phys. Rev. Lett. **105**, 077001 (2010).
[5] Y. Oreg, G. Refael, and F. von Oppen, Helical Liquids and Majorana Bound States in Quantum Wires, Phys. Rev. Lett. **105**, 177002 (2010).
[6] V. Mourik, K. Zuo, S. M. Frolov, S. R. Plissard, E. P. A. M. Bakkers, and L. P. Kouwenhoven, Signatures of Majorana fermions in hybrid superconductor-semiconductor nanowire devices, Science **336**, 1003 (2012).
[7] A. Das, Y. Ronen, Y. Most, Y. Oreg, M. Heiblum, and H.Shtrikman, Zero-bias peaks and splitting in an Al-InAs nanowire topological superconductor as a signature of Majorana fermions, Nat. Phys. **8**, 887 (2012).
[8] M. T. Deng, C. L. Yu, G. Y. Huang, M. Larsson, P. Caroff, and H. Q. Xu, Anomalous zero-bias conductance peak in a Nb-InSb nanowire-Nb hybrid device, Nano Lett. **12**, 6414 (2012).
[9] H. O. H. Churchill, V. Fatemi, K. Grove-Rasmussen, M. T. Deng, P. Caroff, H. Q. Xu, and C. M. Marcus, Superconductor-nanowire devices from tunneling to the multichannel regime: Zero-bias oscillations and magnetoconductance crossover, Phys. Rev. B **87**, 241401 (2013).
[10] S. M. Albrecht, A. P. Higginbotham, M. Madsen, F. Kuemmeth, T. S. Jespersen, J. Nygård, P. Krogstrup, and C. M. Marcus, Exponential protection of zero modes in Majorana islands, Nature (London) **531**, 206 (2016).
[11] H. Zhang *et al.*, Ballistic Majorana nanowire devices, arXiv:1603.04069.
[12] J. Liu, A. C. Potter, K. T. Law, and P. A. Lee, Zero-Bias Peaks in the Tunneling Conductance of Spin-Orbit-Coupled Superconducting Wires with and without Majorana End States, Phys. Rev. Lett. **109**, 267002 (2012).
[13] D. I. Pikulin, J. P Dahlhaus, M. Wimmer, H. Schomerus, and C. W. J. Beenakker, A zero-voltage conductance peak from weak antilocalization in a Majorana nanowire, New J. Phys. **14**, 125011 (2012).
[14] D. Rainis, L. Trifunovic, J. Klinovaja, and D. Loss, Towards a realistic transport modeling in a superconducting nanowire with Majorana fermions, Phys. Rev. B **87**, 024515 (2013).
[15] D. Roy, N. Bondyopadhaya, and S. Tewari, Topologically trivial zero bias conductance peak in semiconductor Majorana wires from boundary effects, Phys. Rev. B **88**, 020502(R) (2013).
[16] E. Zhao, T. Lofwander, and J. A. Sauls, Nonequilibrium superconductivity near spin active interfaces, Phys. Rev. B **70**, 134510 (2004).
[17] A. Cottet and W. Belzig, Conductance and current noise of a superconductor/ferromagnet quantum point contact, Phys. Rev. B **77**, 064517 (2008).
[18] A. Wallraff, D. I. Schuster, A. Blais, L. Frunzio, R.-S. Huang, J. Majer, S. Kumar, S. M. Girvin, and R. J. Schoelkopf, Strong coupling of a single photon to a superconducting qubit using circuit quantum electrodynamics, Nature (London) **431**, 162 (2004).
[19] M. Trif and Y. Tserkovnyak, Resonantly Tunable Majorana Polariton in a Microwave Cavity, Phys. Rev. Lett. **109**, 257002 (2012).
[20] A. Cottet, T. Kontos, and B. Douçot, Squeezing light with Majorana fermions, Phys. Rev. B **88**, 195415 (2013).
[21] T. L.Schmidt, A. Nunnenkamp, and C. Bruder, Microwave-controlled coupling of Majorana bound states, New J. Phys. **15**, 025043 (2013).
[22] O. Dmytruk, M. Trif, and P. Simon, Cavity quantum electrodynamics with mesoscopic topological superconductors, Phys. Rev. B **92**, 245432 (2015).
[23] P. Virtanen and P. Recher, Microwave spectroscopy of Josephson junctions in topological superconductors, Phys. Rev. B **88**, 144507 (2013).
[24] J. I. Väyrynen, G. Rastelli, W. Belzig, and L. I. Glazman, Microwave signatures of Majorana states in a topological Josephson junction, Phys. Rev. B **92**, 134508 (2015).
[25] F. Hassler, A. R. Akhmerov, and C. W. J. Beenakker, The top-transmon: A hybrid superconducting qubit for parity-protected quantum computation, New J. Phys. **13**, 095004 (2011).
[26] T. Hyart, B. van Heck, I. C. Fulga, M. Burrello, A. R. Akhmerov, and C. W. J. Beenakker, Flux-controlled quantum computation with Majorana fermions, Phys. Rev. B **88**, 035121 (2013).
[27] C. Müller, J. Bourassa, and A. Blais, Detection and manipulation of Majorana fermions in circuit QED, Phys. Rev. B **88**, 235401 (2013).
[28] Z.-Y. Xue, L. B. Shao, Y. Hu, S.-L. Zhu, and Z. D. Wang, Tunable interfaces for realizing universal quantum computation with topological qubits, Phys. Rev. A **88**, 024303 (2013).
[29] D. Pekker, C.-Y. Hou, V. E. Manucharyan, and E. Demler, Proposal for Coherent Coupling of Majorana Zero Modes and Superconducting Qubits Using the 4π Josephson Effect, Phys. Rev. Lett. **111**, 107007 (2013).
[30] E. Ginossar and E. Grosfeld, Microwave transitions as a signature of coherent parity mixing effects in the Majorana-transmon qubit, Nat. Commun. **5**, 4772 (2014).
[31] C. Ohm and F. Hassler, Microwave readout of Majorana qubits, Phys. Rev. B **91**, 085406 (2015).
[32] K. Yavilberg, E. Ginossar, and E. Grosfeld, Fermion parity measurement and control in Majorana circuit quantum electrodynamics, Phys. Rev. B **92**, 075143 (2015).
[33] A. Cottet, T. Kontos, and B. Douçot, Electron-photon coupling in mesoscopic quantum electrodynamics, Phys. Rev. B **91**, 205417 (2015).
[34] C. Janvier, L. Tosi, L. Bretheau, Ç. Ö. Girit, M. Stern, P. Bertet, P. Joyez, D. Vion, D. Esteve, M. F. Goffman,

H. Pothier, and C. Urbina, Coherent manipulation of Andreev states in superconducting atomic contacts, Science 2015) 1199 ,**349**).

[35] L. E. Bruhat, J. J. Viennot, M. C. Dartiailh, M. M. Desjardins, T. Kontos, and A. Cottet, Cavity Photons as a Probe for Charge Relaxation Resistance and Photon Emission in a Quantum Dot Coupled to Normal and Superconducting Continua, Phys. Rev. X **6**, 021014 (2016).

[36] T. W. Larsen, K. D. Petersson, F. Kuemmeth, T. S. Jespersen, P. Krogstrup, J. Nygård, and C. M. Marcus, Semiconductor-Nanowire-Based Superconducting Qubit, Phys. Rev. Lett. **115**, 127001 (2015).

[37] G. de Lange, B. van Heck, A. Bruno, D. J. van Woerkom, A. Geresdi, S. R. Plissard, E. P. A. M. Bakkers, A. R. Akhmerov, and L. DiCarlo, Realization of Microwave Quantum Circuits Using Hybrid Superconducting-Semiconducting Nanowire Josephson Elements, Phys. Rev. Lett. **115**, 127002 (2015).

[38] See Supplemental Material at http://link.aps.org/supplemental/10.1103/PhysRevLett.118.126803, which includes Refs. [39–44], for details on our Keldysh approach and the definitions of $\chi(t)$ and $\hat{h}_{\mathcal{R}}$. The Supplemental Material also discusses the case of a microwave cavity coupled to a spin-degenerate Andreev dot or to a quantum dot contacted to a superconductor and subject to a Zeeman field. It finally gives an alternative derivation for the absence of microwave transitions inside a Majorana doublet in the presence of dissipation.

[39] M. L. Goldberger and K. M. Watson, *Collision Theory* (Wiley, New York, 1964).

[40] C. J. Bolech and E. Demler, Observing Majorana Bound States in p-Wave Superconductors Using Noise Measurements in Tunneling Experiments, Phys. Rev. Lett. **98**, 237002 (2007).

[41] S. Tewari, C. Zhang, S. D. Sarma, C. Nayak, and D.-H. Lee, Testable Signatures of Quantum Nonlocality in a Two-Dimensional Chiral p-Wave Superconductor, Phys. Rev. Lett. **100**, 027001 (2008).

[42] S. Walter, T. L. Schmidt, K. Bø rkje, and B. Trauzettel, Detecting Majorana bound states by nanomechanics, Phys. Rev. B **84**, 224510 (2011).

[43] K. Flensberg, Tunneling characteristics of a chain of Majorana bound states, Phys. Rev. B **82**, 180516(R) (2010).

[44] J. Sköldberg, T. Löfwander, V. S. Shumeiko, and M. Fogelström, Spectrum of Andreev Bound States in a Molecule Embedded inside a Microwave-Excited Superconducting Junction, Phys. Rev. Lett. **101**, 087002 (2008).

[45] E. J. H. Lee, X. Jiang, R. Aguado, G. Katsaros, C. M. Lieber, and S. De Franceschi, Zero-Bias Anomaly in a Nanowire Quantum Dot Coupled to Superconductors, Phys. Rev. Lett. **109**, 186802 (2012).

[46] For simplicity, we use a Γ_b which is constant with E_z.

[47] T. D. Stanescu, R. M. Lutchyn, and S. D. Sarma, Dimensional crossover in spin-orbit-coupled semiconductor nanowires with induced superconducting pairing, Phys. Rev. B **87**, 094518 (2013).

[48] M. Schiró and K. Le Hur, Tunable hybrid quantum electrodynamics from nonlinear electron transport, Phys. Rev. B **89**, 195127 (2014).

[49] B. K. Agarwalla, M. Kulkarni, S. Mukamel, and D. Segal, Tunable photonic cavity coupled to a voltage-biased double quantum dot system: Diagrammatic nonequilibrium Green's function approach, Phys. Rev. B **94**, 035434 (2016).

[50] B. K. Agarwalla, M. Kulkarni, S. Mukamel, and D. Segal, Giant photon gain in large-scale quantum dot-circuit QED systems, Phys. Rev. B **94**, 121305(R) (2016).

[51] S. K. Lam, A. Pitrou, and S. Seibert, in *Proceedings of the Second Workshop on the LLVM Compiler Infrastructure in HPC (LLVM '15)* (ACM, New York, 2015).

[52] In practice, the coupling between the fermionic reservoirs and the cavity photons can be characterized by tuning the nanocircuit in the adiabatic regime where tunneling is much faster than ω_0 and using a strong semiclassical microwave excitation, along the lines of Ref. [53].

[53] M. R. Delbecq, L. E. Bruhat, J. J. Viennot, S. Datta, A. Cottet, and T. Kontos, Photon mediated interaction between distant quantum dot circuits, Nat. Commun. **4**, 1400 (2013).

[54] Decoherence could reduce the visibility of an internal transition between two nanowire states. However, the width of feature ① provides an upper bound for the MBS broadening. If feature ① is observable and mediated by the coupling constant β, it implies that the internal transition at $\omega_0 = 2\varepsilon$ will also be visible in the absence of the self-adjoint property.

[55] N. Samkharadze, A. Bruno, P. Scarlino, G. Zheng, D. P. DiVincenzo, L. DiCarlo, and L. M. K. Vandersypen, High Kinetic Inductance Superconducting Nanowire Resonators for Circuit QED in a Magnetic Field, Phys. Rev. Applied **5**, 044004 (2016).

[56] J. Stehlik, Y.-Y. Liu, C. M. Quintana, C. Eichler, T. R. Hartke, and J. R. Petta, Fast Charge Sensing of a Cavity-Coupled Double Quantum Dot Using a Josephson Parametric Amplifier, Phys. Rev. Applied **4**, 014018 (2015).

[57] W. Chang, S. M. Albrecht, T. S. Jespersen, F. Kuemmeth, P. Krogstrup, J. Nygård, and C. M. Marcus, Hard gap in epitaxial semiconductor-superconductor nanowires, Nat. Nanotechnol. **10**, 232 (2015).

[58] A. Palacios-Laloy, F. Nguyen, F. Mallet, P. Bertet, D. Vion, and D. Esteve, Tunable resonators for quantum circuits, J. Low Temp. Phys. **151**, 1034 (2008).

[59] M. Sandberg, C. M. Wilson, F. Persson, T. Bauch, G. Johansson, V. Shumeiko, T. Duty, and P. Delsing, Tuning the field in a microwave resonator faster than the photon lifetime, Appl. Phys. Lett. **92**, 203501 (2008).

[60] J. J. Viennot, M. C. Dartiailh, A. Cottet, and T. Kontos, Coherent coupling of a single spin to microwave cavity photons, Science **349**, 408 (2015).

[61] Y.-Y. Liu, J. Stehlik, C. Eichler, M. J. Gullans, J. M. Taylor, and J. R. Petta, Semiconductor double quantum dot micromaser, Science **347**, 285 (2015).

[62] J. J. Viennot, M. R. Delbecq, M. C. Dartiailh, A. Cottet, and T. Kontos, Out-of-equilibrium charge dynamics in a hybrid circuit quantum electrodynamics architecture, Phys. Rev. B **89**, 165404 (2014).

[63] A. Stockklauser, V. F. Maisi, J. Basset, K. Cujia, C. Reichl, W. Wegscheider, T. Ihn, A. Wallraff, and K. Ensslin, Microwave Emission from Hybridized States in a Semiconductor Charge Qubit, Phys. Rev. Lett. **115**, 046802 (2015).

[64] M. R. Delbecq, V. Schmitt, F. D. Parmentier, N. Roch, J. J. Viennot, G. Fève, B. Huard, C. Mora, A. Cottet, and

T. Kontos, Coupling a Quantum Dot, Fermionic Leads, and a Microwave Cavity on a Chip, Phys. Rev. Lett. **107**, 256804 (2011).

[65] T. Frey, P. J. Leek, M. Beck, A. Blais, T. Ihn, K. Ensslin, and A. Wallraff, Dipole Coupling of a Double Quantum Dot to a Microwave Resonator, Phys. Rev. Lett. **108**, 046807 (2012).

[66] K. D. Petersson, C. G. Smith, D. Anderson, P. Atkinson, G. A. C. Jones, and D. A. Ritchie, Charge and spin state readout of a double quantum dot coupled to a resonator, Nano Lett. **10**, 2789 (2010).

[67] K. D. Petersson, L. W. McFaul, M. D. Schroer, M. Jung, J. M. Taylor, A. A. Houck, and J. R. Petta, Circuit quantum electrodynamics with a spin qubit, Nature (London) **490**, 380 (2012).

[68] Y.-Y. Liu, K. D. Petersson, J. Stehlik, J. M. Taylor, and J. R. Petta, Photon Emission from a Cavity-Coupled Double Quantum Dot, Phys. Rev. Lett. **113**, 036801 (2014).

[69] C. J. Bolech and E. Demler, Observing Majorana Bound States in p-Wave Superconductors Using Noise Measurements in Tunneling Experiments, Phys. Rev. Lett. **98**, 237002 (2007).

[70] J. Nilsson, A. R. Akhmerov, and C. W. J. Beenakker, Splitting of a Cooper Pair by a Pair of Majorana Bound States, Phys. Rev. Lett. **101**, 120403 (2008).

[71] J. Liu, F.-C. Zhang, and K. T. Law, Majorana Fermion induced non-local current correlations in spin-orbit coupled superconducting wires, Phys. Rev. B **88**, 064509 (2013).